XLI CILAMCE
XLI Ibero-Latin American Congress on Computational Methods in Engineering
16-19 November, 2020 FOZ DO IGUAÇU PARANÁ - BRAZIL

Fatigue analysis of gravity-based foundation supporting a 10 MW OWT considering small-strain stiffness of soils

Eduardo Dorscheidt[1], Fellipe A. Gomes[1], Gabriel Nogueira[1], Gilberto B. Ellwanger[1]

[1]*Dept. of Civil Engineering, Federal University of Rio de Janeiro*
Av. Athos da Silveira Ramos, 149, 21941-909, Ilha do Fundão, Rio de Janeiro, Brazil
eduardo.dorscheidt@coc.ufrj.br, fellipe.gomes@coc.ufrj.br, gabrielnogueira@coc.ufrj.br, gbe@coc.ufrj.br

Abstract. In the past few years, gravity-based foundations (GBF) proved to be an advantageous solution for supporting offshore wind turbines (OWT) when soil conditions represent a hindrance to deep foundations as monopiles. In this type of support structure, soil-structure interaction (SSI) interferes directly in system stiffness. The available standard formulations are still based on the Theory of Elasticity and do not contemplate some soil properties, as its hardening effects when subjected to plastification. This paper aimed to investigate the influence of an elasto-plastic soil model such as HSS (Hardening Soil with Small-Strain Stiffness) in a coupled fatigue analysis of concrete, a critical point of GBF structural design, considering a 10 MW OWT. The results of the proposed analysis showed low influence of small-strain stiffness, but a significant role of plasticity and hardening effects.

Keywords: gravity-based foundation, soil-structure interaction, hardening soil, offshore wind turbine.

1 Introduction

A worldwide trend is to transfer the investments in wind energy to the offshore environment, as has been shown in many technical reports year by year (Wind Europe [1]; Beiter *et al.* [2]; The Carbon Trust [3]). This tendency is mainly based on the fact that offshore wind turbines (OWT) can take advantage of stronger and more uniform winds as opposed to the ones in the onshore environment, which has complex logistical matters to install high power-rating turbines. Almost thirty years ago, the first fashion of support structure of OWT was the gravity-based foundation (GBF). It has been in use since 1991 in Denmark to support 500 kW wind turbines. However, because of its massive weight causing difficulties in transport and installation, they lost competitiveness for steel monopiles in the first decade of this century. Nevertheless, since Thorntonbank I (Belgium, 2009) lighter models of GBF were presented, making it again a competitive support solution (DORSCHEIDT [4]).

Esteban, López-Gutiérrez and Negro [5] elaborated a state-of-the-practice report of GBF until the Elisa-ELICAN project, which was installed in 2018 in Spain. Despite not been mentioned in this paper, the other recent offshore wind farm over GBF was Blyth, also a demonstrator project installed in 2017 in the UK (DORSCHEIDT [4]). Both offshore wind projects are up to 35-40 m depth sea level, what is meaningly deeper than the sea levels explored until the previous wind farm using gravity-based foundation, which was Kårehamn (Sweden, 2013) up to 20 m depth. Recent researches, such as Koekkoek [6], Nadal [7], and Dorscheidt [4], show the viability of lighter new models of GBF applied to deeper sea levels.

Koekkoek [6] and Dorscheidt [4] proposed the soil-structure interaction (SSI) analysis of these lighter models of gravity-based foundations, by different methodologies. The main reason for these analyses is that the standard approaches of SSI in these structures are based on classic elastic spring models traced for foundations way different than GBF of offshore wind turbines. Dorscheidt [4], who focused on create nonlinear springs from Finite Element Method (FEM) models, demonstrate that, in a coupled analysis, the use of the elastic-linear spring can underestimate the value of displacements in 20% when compared to an elasto-plastic approach using hardening soil constitutive model. This article focuses on extending these SSI analyses of a gravity-based foundation supporting a 10 MW offshore wind turbine using the Hardening Soil with Small-strain stiffness (HSS) model to

investigate the soil influence in the structural fatigue of the foundation.

1.1 Problem description

Fatigue is a primary concern in the structural design of support structures for offshore wind turbines. Since soil-structure interaction exerts substantial influence in foundations like GBFs because of its large direct contact area between soil and concrete, the different modelling fashions can imply in divergent responses. The aim of this paper is to compare the elastic-linear spring model proposed by DNVGL [8] with a set of springs calibrated by a FEM model using HSS constitutive model in Plaxis 3D in terms of concrete's fatigue response in a gravity-based foundation.

1.2 Available approaches

A widespread method for SSI in shallow foundations of structures subjected to vibrations was proposed by Gazetas [9], replayed by Barltrop and Adams [10] and present in DNV standards since 1992 [11]. Now-a-days, it is found in DNVGL-RP-C212 [8] in the same section (Sec. 8) that recommends the benefits of a FEM analysis. Figure 1 shows the set of springs adopted in the model and Table 1 presents their formulations, where G is the elastic shear modulus, R is the foundation radius and ν is Poisson's ratio. This paper does not evaluate SSI damping coefficients also proposed by DNVGL [8]. Some discussion about this task can be found in Dorscheidt [4].

Table 1. Spring coefficients proposed by DNVGL-RP-C212 [8].

Mode of motion	Vertical	Horizontal	Rotation
Spring coefficient (K)	$\frac{4GR}{1-\nu}$	$\frac{8GR}{2-\nu}$	$\frac{8GR^3}{3(1-\nu)}$

With respect to the fatigue damage calculation, Palgreen-Miner's rule was applied in association with the SN curve proposed by DNVGL-ST-C502 [12], which is widely used and produces conservative results as stated in Gomes [13]. As for the stress-cycle counting, WAFO toolbox [14] is used to identify the local maximums in the compression-compression zone. For further information regarding the applied methodology, the authors recommend the work of Nadal [7], Gomes [13] and Nogueira *et al.* [15].

2 Proposed model

Through a coupled analysis performed by SIMA-RIFLEX, the authors evaluate the influence of the SSI model in a gravity-based foundation supporting a 10 MW wind turbine, whose properties can be found in Bak *et al.* [16]. Validations made around this model and software are available in Nogueira [17].

2.1 Structural model

Table 2 shows the geometrical properties of the structural model. For the steel tower, it was considered a density of 8500 kg/m³, Young's modulus of 210 GPa and 0.3 for Poisson's ratio. For the concrete foundation, it was assumed a characteristic strength of 40 MPa and 0.2 for Poisson's ratio. The remaining material properties were taken from criteria defined by Brazilian recommended practice ANBT NBR 6118:2014 [18]. The structural model in SIMA-RIFLEX can be better understood in Fig. 1. The complete validation of this model can be found in Nogueira *et al.* [15].

Table 2. Dimensions of the structural model

Section	Length [m]	Ext. diameter [m]	Thickness [m]
Tower	110.63	5.5 – 8.3	0.02 – 0.038
Dry shaft	5.00	8.3	1.00
Submerged shaft	26.50	8.3	1.00
Base (top)	-	35.0	1.50
Base (central)	13.5	35.0	1.00
Base (bottom)	-	35.0	1.50

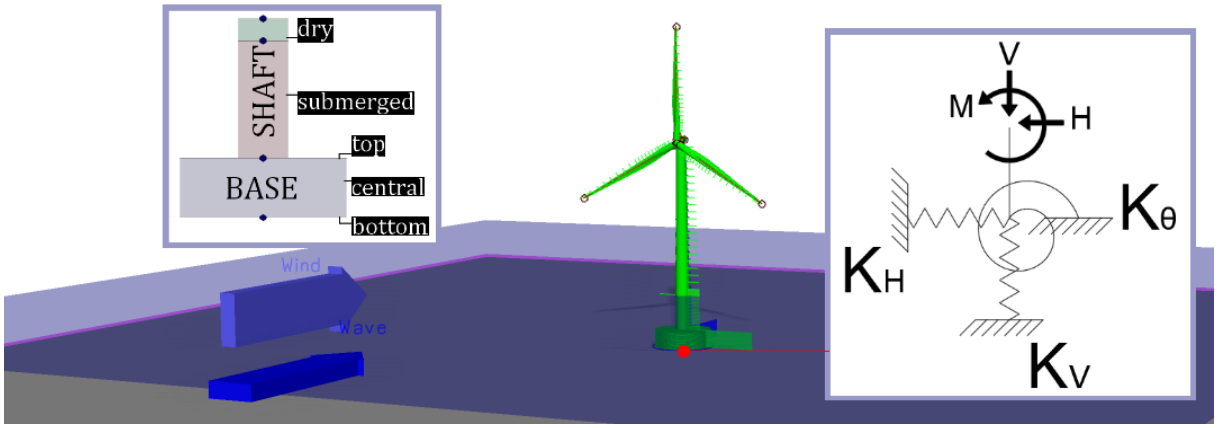

Figure 1. Structural model of the 10 MW OWT over gravity-based foundation using a set of springs to represent SSI in SIMA-RIFLEX.

2.2 FEM approach for soil modeling

As recommended by DNVGL (2017) [8], whenever possible, the Finite Element Method shall be used to evaluate soil-structure interaction problems. The use of this numerical modelling introduces a bunch of benefits, such as the possibility of implementing advanced elasto-plastic soil models and the possibility of including layered soils and drainage conditions. The SSI model in Plaxis 3D consists of frame elements to represent the wind turbine tower and nacelle, shell elements modelling the GBF itself, and volumetric elements to model the soil. In Plaxis, the volumetric element available is a tetrahedral element with ten nodes and four integration points, which is indicated by Fig. 2.

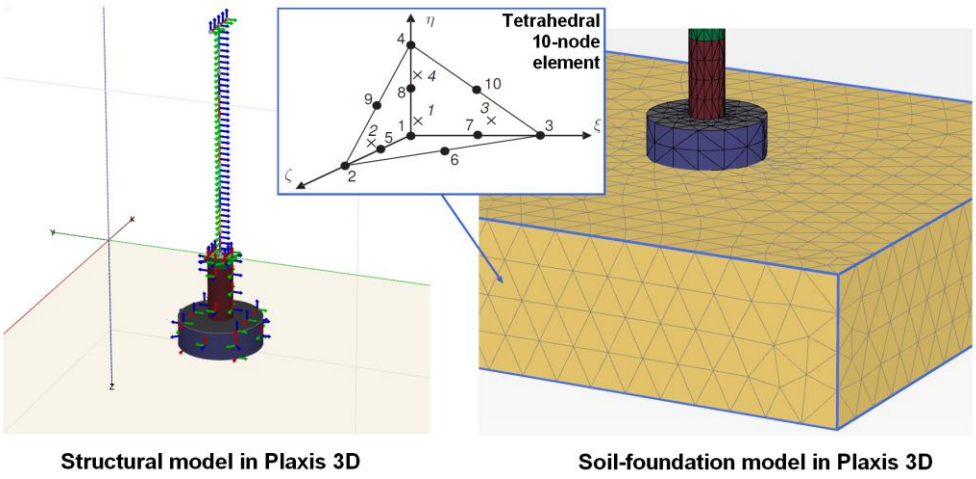

Figure 2. FEM proposed model in Plaxis 3D.

2.3 Elasto-plastic constitutive models

An elasto-plastic constitutive model has a material behavior that does not obey Hooke's Law for every range of loading. According to Potts and Zdravkovic [19] and Helwany [20] there are three main elasto-plastic behaviors in soils: the elastic perfectly plastic model, the hardening model, and the softening model, the latter being mainly applied in soft clays and therefore out of the aim of this paper. The perfectly plastic model can be observed in Fig. 3, where the material behavior obeys an only slope governed by elastic Young's modulus (A-B line). Once the curve reaches the stress σ_y (point B), it develops a perfectly plastic behavior until rupture.

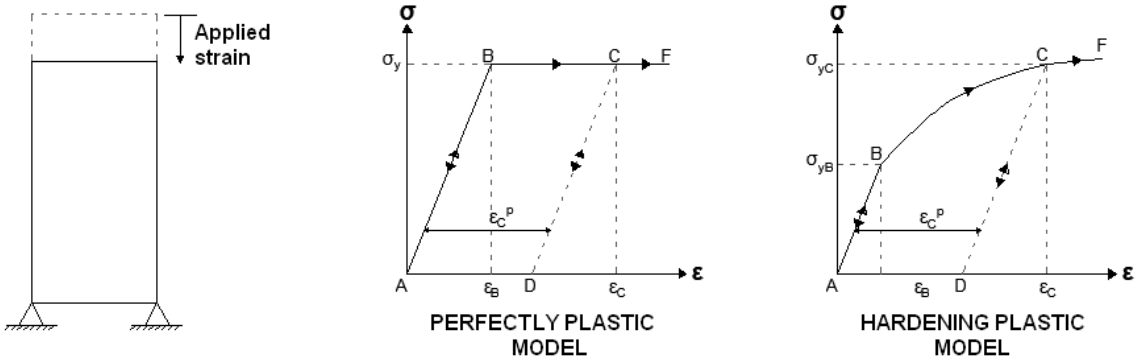

Figure 3. Idealized behavior of a perfectly plastic and a hardening plastic model after a uniaxial loading [19].

A perfectly plastic model widely used in soil modelling is the Mohr-Coulomb model, where σ_y can be understood as the stress related to the ultimate load (i.e., p_u in a $p - y$ curve). According to Dorscheidt [4], Çelik [21], and Hsiung and Dao [22] this property makes Mohr-Coulomb a conservative model, as a perfectly plastic behavior overestimates the displacements of both shallow and deep foundations.

Another possible material behavior is shown at the right graphic of Fig. 3: the (uniaxial) hardening plastic behavior. Just like the Mohr-Coulomb model, point B still delimitates the beginning of the plastic behavior, but instead of a large strain until rupture, the material yields until point C. This new segment B-C is what characterizes the hardening plastic behavior. The slope in this new segment decreases from B to C, which means that soil becomes less hard up to reach point C, when it becomes likely to failure at any stress increment (point F).

2.4 Hardening soil with small-strain stiffness (HSS)

Kondner (1963) [23] was who first observed through undrained triaxial tests that when subjected to primary deviatoric loading, after reaching plasticity, soil (stiff or soft) shows a decreasing stiffness that can be approximated by a hyperbola. This behavior was then formulated as the hyperbolic-model by Duncan and Chang (1970) [24]. Schanz, Vermeer and Bonnier (1998) [25] applied this formulation to propose the Isotropic Hardening Soil model, also known as Standard Hardening Soil model (PLAXIS [26]). The construction of the hyperbola depends on the use of three stiffness moduli, whose guidance can be found in Plaxis manuals [26] and Obrzud and Truty [27] (the index ref indicates reference values according to a reference stress (p^{ref}), 100 MPa by Plaxis' default [26]): E_{50}^{ref}, the (reference) secant stiffness in standard drained triaxial test; E_{oed}^{ref}, the (reference) tangent stiffness for primary oedometer loading; E_{ur}^{ref}, the (reference) unloading / reloading stiffness.

A series of hardening plastic models are available nowadays to describe the behavior of elasto-plastic materials. Benz [28] proposed a hardening model that was incorporated to Plaxis 3D in the past years to better represent the phenomena of extra stiffness in soils for small-strains ($\gamma < 10^{-3}$). The Hardening Soil with Small-strain Stiffness (HSS) is a total nonlinear elasto-plastic model that can well represent real soil behavior in many different applications, especially when soil is submitted to cycles of small stresses (BRINKGREVE *et al.* [29]). Compared to Standard Hardening Soil model, HSS uses two additional parameters: the so-called very small-strain shear modulus (G_0), which is usually obtained by isotropic relation with initial E_0, and the shear strain $\gamma_{0.7}$ at which the secant shear modulus is reduced to 72.2% of G_0, percentage proposed by Santos and Correia [30] for small-strain hyperbolic law formulated by Hardin and Drnevich [31], based on the already mentioned Kondner's

hyperbolic law for larger strains (PLAXIS [26]). The complete formulation of this model can be found in Benz [28].

For the proposed analysis, the soil parameters were taken from the tutorial manual of Plaxis 3D [32], which is an open-source reference, whose properties are presented in Table 3. It is valid to stand out that these parameters are similar to sands found in some locations around the Brazilian coast.

Table 3. Non-cohesive soil parameters used for the HSS model.

Parameter	γ_{un} [kN/m³]	γ_{sat} [kN/m³]	c' [kN/m²]	φ' [deg]	ψ' [deg]	m [-]	ν' [-]	$\gamma_{0,7}$ [-]	G_0^{ref} [MPa]
Value	19	20	5	28	0	0,5	0,2	1.5×10^{4}	100

2.5 Loading conditions

In the proposed analysis, the turbulent-wind simulator TurbSim (JONKMAN [33]) was employed to create realistic aerodynamic forces. Kaimal Spectrum was used, considering a turbulence intensity (TI) equal to 5.9% and a power-law exponent (α) equal to 0.056, according to Sakagami [34] considering data from Brazilian Northeast's shore. Airy's wave theory represented the cinematics of the irregular waves in Jonswap Spectrum. The MacCamy-Fuchs load model was used to calculate the hydrodynamic forces. All loading parameters can be found in Nogueira *et al.*[15]. The twelve loading cases are presented in Table 3:

Table 4. FLS loading cases and their occurrences [17]

Case	Direction	U_{10} (m/s)	H_S (m)	T_P (s)	Occurrence (%)
1	N	5	0.7	3.6	0.21
2	NE	7	1.2	4.6	2.15
3	E	9	1.6	5.4	21.86
4	E	12	2.2	6.3	13.82
5	E	13	2.4	6.6	9.08
6	SE	8	0.7	3.4	22.52
7	SE	10	0.9	3.7	16.87
8	SE	11	1.0	3.9	12.17
9	S	6	0.4	2.7	1.13
10	SW	5	0.4	2.6	0.08
11	W	5	0.7	3.6	0.05
12	NW	5	0.7	3.6	0.06

3 Results

The results obtained for fatigue assessment of both elastic-linear (DNVGL method) and the HSS model are presented in Table 4. The values of damage shown are not multiplied by its occurrence frequency. Thus it is possible to visualize the pure response resulted from each one of the twelve loading cases.

Table 5. Response for the twelve loading cases in the critical point of GBF's slab.

Cases	Ca.1	Ca.2	Ca.3	Ca.4	Ca.5	Ca.6	Ca.7	Ca.8	Ca.9	Ca.10	Ca.11	Ca.12
DNVGL	1.01×10^{-5}	5.67×10^{-4}	5.24×10^{-2}	2.06×10^{-2}	1.17×10^{-2}	2.25×10^{-4}	1.78×10^{-2}	8.00×10^{-3}	2.85×10^{-5}	1.02×10^{-5}	1.01×10^{-5}	1.01×10^{-5}
HSS	1.17×10^{-5}	6.16×10^{-4}	5.24×10^{-2}	2.33×10^{-2}	1.13×10^{-2}	2.46×10^{-4}	1.84×10^{-2}	8.14×10^{-3}	3.19×10^{-5}	1.14×10^{-5}	1.17×10^{-5}	1.17×10^{-5}
Variat.	17%	8%	0.02%	13%	9%	9%	3%	1.7%	12%	12%	16%	16%

Analyzing the range of variation in the last line of Table 4, it becomes clear that different load cases provide different margins of variation between an elastic-linear spring and a hardening elasto-plastic spring. A series of

variables are involved in comparing one case response with another, e.g., wind speed, wave significant height (H_s), wave peak period (T_p), the direction of loads, the position of the critical point in the GBF, and any other parameter that can influence stress assessment. When compared with an elastic-linear curve, HSS model has a more rigid curve segment in its start and a more flexible segment after reaching a stress-strain relation around E_{50}. This means, for instance, that Case 3 is a loading case that is exciting a SSI stiffness quasi-elastic, which explains why its response is nearly equal for elastic-linear spring and HSS model. Case 3 is the critical case; thus, the lifetime assessment of both models shall be almost the same.

When multiplied by frequency, the elastic-linear spring model resulted in 65 years of lifetime in the critical point of GBF's shaft, two years higher than the result found for the HSS model. More examples of lifetime results of the elastic-linear model can be found in Nogueira *et al.* [15].

4 Conclusions

This paper aimed at investigating the influence of an elasto-plastic SSI model considering small-strain stiffness. Despite some references showing the notable effect of hardening models in displacements evaluation, the final result of the proposed analysis pointed to a low influence in the fatigue lifetime. However, there are two central remarks:

- The lifetime variation was low because the critical case (Case 3) had a condition set prone to it, as shown in Table 4. After multiplied by its occurrence frequency, Case 3 might no longer be the critical one, and the lifetime variation could be much higher.
- Every column result in Table 4 showed a higher value of damage in the HSS model. This proves that the property of small-strain stiffness was not significant for the condition sets, since the majority of stresses in soil probably did not produce small strains ($< 10^{-3}$). Thus, as it was observed in Dorscheidt [4], only the Standard Hardening Soil model would be enough to evaluate the SSI problem of an OWT over a gravity-based foundation.

Acknowledgements. The study described in this paper is the result of a partnership between Petrobras and UFRJ and was carried out with resources from the R&D program of the Electricity Sector regulared by ANEEL, under the PD-00553-0045/2016 project titled "Planta Piloto de Geração Eólica Offshore". The authors would also like to express their gratitude to "Coordenação de Aperfeiçoamento de Pessoal de Nível Superior" (CAPES) and "Conselho Nacional de Desenvolvimento Científico e Tecnológico" (CNPq) for the resources destined to the production of this research.

Authorship statement. The authors hereby confirm that they are the sole liable persons responsible for the authorship of this work, and that all material that has been herein included as part of the present paper is either the property (and authorship) of the authors, or has the permission of the owners to be included here.

References

[1]. Wind Europe, *Wind energy in Europe in 2019: Trends and statistics*, 2020.

[2]. P. Beiter *et al.*, *An assessment of the economic potential of offshore wind in the United States from 2015 to 2030*. National Renewable Energy Laboratory, 2017.

[3]. The Carbon Trust, *Offshore wind industry review of GBSs*: Identifying the key barriers to large scale commercialization of gravity-based structures (GBSs) in the offshore wind industry. The Scottish Government, 2015.

[4]. E. Dorscheidt, *Interação solo-estrutura de turbinas eólicas offshore sobre fundação de gravidade*. MSc thesis, Federal University of Rio de Janeiro, 2020.

[5]. M. D. Esteban, J. S., Lópes-Gutiérrez and V. Negro, "Gravity-based foundations in the offshore wind sector". *Journal of Marine Science and Engineering*, v.7, pp. 64-73, 2019.

[6]. R. Koekkoek, *Gravity base foundations for offshore wind turbines.* MSc thesis, Delft University of Technology, 2015.

[7]. A. O. Nadal, *Time domain simulation parameters for fatigue assessment of an offshore gravity based wind turbines.* MSc thesis, Norwegian University of Science and Technology, 2018.

[8]. DNVGL-RP-C212, *Offshore soil mechanics and geotechnical engineering.* Det Norske Veritas Germanischer Lloyd, 2017.

[9]. G. Gazetas, *Analysis of machine foundation vibrations: State of the art*, Soil Dynamics and Earthquakes Engineering, v. 2, n. 1, 1983.

[10]. N. Barltrop and A. Adams, *Dynamics of fixed marine structures*. 3 ed. Epsom, Atkins Oil & Gas Engineering Limited, 1991.

[11]. DNV Classification notes no. 30.4, *Foundations*. Det Norske Veritas, 1992.

[12]. DNVGL-ST-C502, *Offshore concrete structures.* Det Norske Veritas Germanischer Lloyd, 2018.

[13]. F. A. Gomes, *Análise de fadiga de turbinas eólicas offshore do tipo monopile com conexão grauteada*. MSc thesis, Federal University of Rio de Janeiro, 2019.

[14]. Brodtkorb, P. A. *et al*. WAFO a Matlab toolbox foy analysis of random waves and loads. In: *Tenth International Offshore and Polar Engineering Conference*, International Society of Offshore and Polar Engineers, 2000.

[15]. G. Nogueira, *et al. Design and fatigue assessment of gravity base foundaitons for offshore wind turbine.* ", In: Proceedings of XLI CILAMCE, 2020.

[16]. C. Bak, *et al.*, *Description of the DTU 10 MW reference wind turbine.* Danmarks Tekniske Universitet, 2013.

[17]. G. Nogueira, *Avaliação do comportamento de turbinas eólicas offshore fixas do tipo monopile.* MSc thesis, Federal University of Rio de Janeiro, 2019.

[18]. ABNT NBR 6118, *Projeto de estruturas de concreto – Procedimento.* Associação Brasileira de Normas Técnicas, 2014.

[19]. D. M. Potts and L. Zdravkovic, *Finite element analysis in geotechnical engineering.* Thomas Telford Publishing, 1999.

[20]. S. Helwany, *Applied soil mechanics with ABAQUS applications.* John Wiley & Sons, 2007.

[21]. S. Çelik, "Comparison of Mohr-Coulomb and hardening soil models numerical estimation of ground surface settlements caused by tunneling". *Igdur Universitesi Bilimleri Enstitusu Dergisi*, v.7, n. 4, pp. 95-102, 2017.

[22]. B. C. B. Hsiung and S. D. Dao, "Evaluation of constitutive soil models for predicting movements caused by a deep excavation in sands". *Eletronic Journal of Geotechnical Engineering*, v. 19, pp. 17326-17344, 2014.

[23]. R. Kondner, "A hyperbolic stress strain formulation for sands", In: Proceedings of the Pan. Am. ICOSFE Brazil, 1963.

[24]. J. M. Duncan and C. Y. Chang, "Nonlinear analysis of stresses and strain in soil". *ASCE Journal of Soil Mechanics and Foundations*, v. 96, pp. 1629-1653, 1970.

[25]. T. Schanz, P. A. Vermeer and P. G. Bonnier, "The Hardening Soil model: formulation and verification". In: R. B. J. Brinkgreve (ed.), *Beyond 2000 in Computational Geotechnics*. Balkema, 1999.

[26]. Plaxis, *Material models: connect edition V20,* 2019.

[27]. R. F. Obrzud and A. Truty, *The hardening soil model: a practical guidebook.* ZSoil.PC 100701 Report, 2018.

[28]. T. Benz, *Small-strain stiffness of soils and its numerical consequences.* PhD thesis, Institut für Geotechnik der Universität Stuttgart, 2006.

[29]. R. B. J. Brinkgreve *et al.*, "Hysteretic damping in a small-strain stiffness model". In: *Proceedings of the 10th NUMOG*, pp. 737-742, 2007.

[30]. J. A. Santos and A. G. Correia. "Reference threshold shear strain of soil. Its application to obtain a unique strain-dependent shear modulus curve for soil". In: *Proceedings of the 15th ICSMGE*, pp. 267-270, 2001.

[31]. B. O. Hardin and V. P. Drnevich, "Shear modulus and damping in soil: design equations and curves", *ASCE Journal of the Soil Mechanics and Foundations Division*, v. 98, pp. 667-692, 1972.

[32]. Plaxis, *Tutorial manual: connect edition V20,* 2019.

[33]. B. J. Jonkoman, *TurbSim User's Guide: version 1.50*. NREL Technical Report, 2009.

[34]. Y. Sakagami, *Influência da turbulência e do perfil de velocidade do vento no desempenho de aerogeradores em dois parques eólicos na costa do Nordeste Brasileiro*. PhD thesis, Federal University of Santa Catarina, 2017.